One other striking difference between the enthalpic aging data for the blend and that for the homopolymer is that while the phenomenological model of Hodge and Berens[12a] can be applied successfully to the homopolymer C_p data, we have been unable to obtain reasonable curve fits to any of the C_p data for the blend. This is believed to be due to the breadth of the glass transition process(es) occurring in the blend (ΔT = 38 K compared with $\Delta T \simeq$ 6 K for a typical homopolymer). We are currently engaged in the (somewhat lengthy) process of analyzing our enthalpic aging data for this and several other polymer systems in terms of the Hodge/Berens phenomenological model and will report the results in a subsequent publication.

Conclusions

Enthalpic aging phenomena in a conditionally miscible blend of polystyrene and poly(vinyl methyl ether) have been analyzed in terms of two models of physical aging in polymer glasses. The results show that aging in the blend is slower than in the case of the lower T_g component. Furthermore, it is suggested that it is the more mobile lower T_g component which appears to be responsible for most of the aging effects measured. We realize, however, that the higher T_g component (polystyrene) must provide a minor contribution to the total aging, although at these temperatures the PS enthalpy relaxation processes should be much slower than those for PVME.

It is thought that enthalpic aging involves the motions of much smaller dynamic units than does the glass transition process. Hence, enthalpic aging could be another useful probe for studying miscibility and immiscibility in polymer blends.

Further work in this area could involve (a) studying the effects of composition on the enthalpic aging process in a blend and (b) the investigation of a more compatible system such as polystyrene/poly(α-methylstyrene) blends.

Acknowledgment. R.F. acknowledges support from the SERC received during the course of this study via a postdoctoral fellowship.

Registry No. PVME, 9003-09-2; PS, 9003-53-6.

References and Notes

(1) Cowie, J. M. G.; Ferguson, R. *Polym. Commun.* **1986**, *27*, 258.
(2) Maurer, F. H. J.; Palmen, J. H. M.; Booij, H. C. *Rheol. Acta* **1985**, *24*, 243.
(3) Cavaille, J. Y.; Etienne, S.; Perez, J.; Monnerie, L.; Johari, G. P. *Polymer* **1986**, *27*, 686.
(4) Kwei, T. K.; Nishi, T.; Roberts, R. F. *Macromolecules* **1974**, *78* 667.
(5) Shibayama, M.; Yang, H.; Stein, R. S. *Macromolecules* **1985**, *18*, 2179.
(6) Cowie, J. M. G.; Ferguson, R. *Macromolecules*, preceding paper in this issue.
(7) Richardson, M. J.; Saville, N. G. *Polymer* **1975**, *16*, 753.
(8) Moynihan, C. T.; Macedo, P. B.; Montrose, C. J.; Gupta, P. K.; DeBolt, M. A.; Dill, J. F.; Dom, B. E.; Drake, P. W.; Easteal, A. J.; Elterman, P. B.; Moeller, R. P.; Sasabe, H. S.; Wilder, A. J. *Ann. N.Y. Acad. Sci* **1976**, *279*, 15.
(9) Press, W. H.; Flannery, B. P.; Teukolsky, S. A.; Vetterling, W. T. *Numerical Recipes: The Art of Scientific Programming*; Cambridge University Press: Cambridge, 1986.
(10) Petrie, S. E. B.; Marshall, A. S. *J. Appl. Phys.* **1975**, *46*, 4223.
(11) Cowie, J. M. G.; Ferguson, R., unpublished results.
(12) (a) Hodge, I. M.; Berens, A. R. *Macromolecules* **1982**, *15*, 762. (b) Hodge, I. M.; Huvard, G. S. *Macromolecules* **1983**, *16*, 371.

Studies of the Antenna Effect in Polymer Molecules. 12. Photochemical Reactions of Several Polynuclear Aromatic Compounds Solubilized in Aqueous Solutions of Poly(sodium styrenesulfonate-*co*-2-vinylnaphthalene)

M. Nowakowska,† B. White, and J. E. Guillet*

Department of Chemistry, University of Toronto, Toronto, Ontario, Canada M5S 1A1.
Received September 27, 1988; Revised Manuscript Received November 14, 1988

ABSTRACT: The solubilization and photochemical reactions of several polynuclear aromatic compounds (PNA) in aqueous solutions of poly(sodium styrenesulfonate-*co*-2-vinylnaphthalene) (PSSS-VN) have been studied. The solubilization of PNA compounds has been shown to be quite efficient in aqueous solutions of PSSS-VN. In the absence of oxygen, irradiation of the aqueous polymer solution containing anthracene led to the photosensitized dimerization reaction. In the presence of oxygen photooxidation of the PNA compounds involving singlet oxygen occurred.

Introduction

Various synthetic polyelectrolytes consisting of hydrophobic and hydrophilic groups have been found to form hydrophobic microdomains within the polymer coil in aqueous solution.[1-10] This conformation enables solubilization of both aliphatic and aromatic hydrocarbons. Moreover, many of the known synthetic polyampholytes exhibit this behavior at low degrees of ionization.

In the previous studies in this series it has been shown that the novel polyelectrolyte poly(sodium styrenesulfonate-*co*-2-vinylnaphthalene) (PSSS-VN) efficiently solubilized large hydrophobic compounds.[9,10] Solubilization was found to be only slightly affected by a change in pH or ionic strength. It has also been shown that PSSS-VN exhibits very promising photocatalytic activity. The polymer sensitizes photochemical reactions of solubilized compounds by absorbing light in the UV–visible spectral region and transferring the excitation energy to the solubilized molecules. It is believed that this phenomenon has potential practical applications.

Many of the polynuclear aromatic compounds (PNA) are thought to be carcinogenic. Although such compounds are only sparingly soluble in water, they can be easily introduced into the human body. Thus the search for a

† On leave from the Faculty of Chemistry, Jagiellonian University, Krakow, Poland.

0024-9297/89/2222-2317$01.50/0

method of removing these substances from polluted water sources is of great interest. Polycyclic compounds dissolved in hydrocarbon solvents are known to undergo photooxidation involving singlet oxygen. The reaction results in the formation of endoperoxides.[11-14] The quantum yield and rate constant of oxygenation vary considerably for different PNA compounds.[14]

The present study deals with photochemical reactions of PNA compounds solubilized in aqueous solutions of PSSS-VN. Because of the high catalytic efficiency and analogy to biological catalysts, which usually contain a hydrophobic reaction center, such polymer systems have been termed "photozymes".

Experimental Section

Materials. Poly(sodium styrenesulfonate-*co*-2-vinylnaphthalene) was synthesized and purified according to the method previously described.[9] The polymer consists of 60 mol % vinylnaphthalene and 40 mol % sodium styrenesulfonate. The weight average molecular weight, $\bar{M}_w$, was determined by the ultracentrifuge method to be 310 000. The number average molecular weight of the polymer was estimated assuming a polydispersity of 2.0.

9,10-Dimethylanthracene (DMA, 99%), 9,10-diphenylanthracene (DPA, 99%), and 9-methylanthracene (MA, 95%) (all Aldrich) were purified by three recrystallizations from ethanol. Anthracene (A) and perylene (P) (99.9%, Aldrich gold label) were used without further purification. 1,3-Diphenylisobenzofuran (DPBF, Aldrich) was recrystallized three times from benzene in dark. Anthraquinone (97%, Aldrich) was recrystallized three times from benzene. 10-Hydroxyanthrone was prepared by the method of Carlson and Hercules.[15]

Polymer solutions were prepared by using deionized water. The ionic strength of the aqueous polymer solutions was adjusted by adding a NaCl solution, and the pH was changed by using standard HCl or NaOH solutions. Ethyl alcohol (anhydrous, Aldrich), acetone and benzene (both spectro grade, Caledon), and tetrahydrofuran (HPLC, Aldrich) were used without purification.

Procedures. Solubilization of Probes. Solubilization of PNA compounds in aqueous polymer solutions was achieved by slowly injecting microliter quantities of probe (1×10^{-2} M) dissolved in acetone to milliliter quantities of polymer solution. The final aqueous polymer solution contained less than 0.1 vol % acetone. The mixture was shaken for 5 min and equilibrated in the dark for 2–4 h.

Irradiation of Samples. Irradiations were carried out by using a deep-UV, constant intensity control system (Optical Associates Model 780) described earlier in detail.[6] A 280-nm interference filter was used to obtain monochromatic light. The incident light intensity was determined by using a ferrioxalate actinometer:[16] $I_0 = 6.86 \times 10^{-7}$ einstein dm^{-3} s^{-1}. Solar-simulated irradiations were performed by using the apparatus described previously.[9]

Ultraviolet Spectra. UV spectra of the samples were measured by using a Hewlett-Packard 8451A diode array spectrophotometer.

Fluorescence Spectra. Steady-state emission and excitation spectra of PSSS-VN solutions were recorded at room temperature on a Spex Fluorolog-2 fluorescence spectrometer. Emission spectra were corrected for the wavelength dependence of the detector response by using an internal correction function provided by the manufacturer. The concentration of the different probes in aqueous solutions of PSSS-VN were calculated from standard plots of the total fluorescence intensity versus concentration of the probe in THF and acetone solutions. Emission of anthracene excimer was recorded at 77 K. This study was accomplished by adding increasing amounts of anthracene to aqueous solution of PSSS-VN and observing changes in the emission profile at excitation at 340 nm.

Transient Measurements of Fluorescence Decay. Fluorescence decay curves were measured with a single-photon-counting apparatus. The solutions were degassed with five freeze–pump–thaw cycles before sealing in quartz tubes.

Viscosity Measurements. Viscosities of the polymer solutions were measured by using an automatic viscometer described earlier.[17] Values of the intrinsic viscosity and effective hydrodynamic volume (V_{eff}) of PSSS-VN in aqueous solution at different pH and ionic strength were determined by using the method described elsewhere.[10]

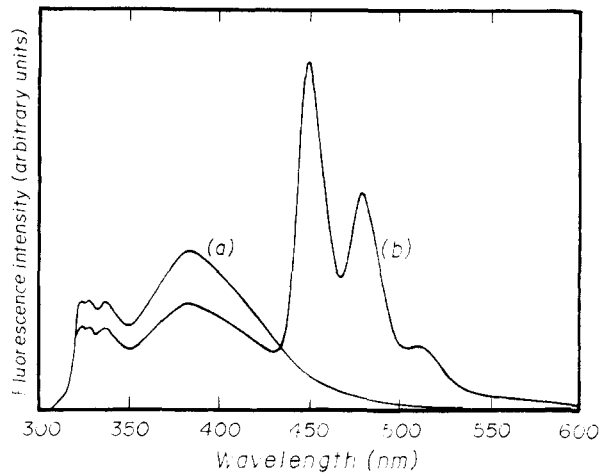

Figure 1. Steady-state fluorescence spectrum of PSSS (40 mol %)-VN in aqueous solution at neutral pH, $c_{pol} = 0.01$ g dm^{-3}, $\lambda_{ex} = 280$ nm (a), and PSSS-VN containing solubilized perylene, $c_p^t = 1.07 \times 10^{-6}$ M (b).

Gas Chromatography Analysis. Analysis of the products formed during irradiation of the different photozymes as well as the self-sensitized autooxidation and dye-sensitized photooxidation of PNA compounds in organic solvents were carried out by using a Varian Aerograph series 1700 gas chromatograph with the temperature programmed (from 150 to 280 °C at 6 °C min^{-1}). The instrument contained a flame ionization detector (FID) and a 6 ft × 2 mm OV17 glass column (5% w/w Carbowax on Chromosorb G) fitted with a glass-wool precolumn. The function of the precolumn was to remove the polymer from the samples, thereby enabling direct analysis of the reaction products. The analyses were based on a comparison of the retention times of the products with the corresponding pure substances.

Results and Discussion

I. Solubilization of Polynuclear Aromatic Compounds. Studies of the solubilization of PNA compounds in aqueous solutions of PSSS-VN were started by using perylene as a fluorescence probe. Perylene was chosen since it is sparingly soluble and exhibits very low emission intensity in water.[18]

The steady-state fluorescence spectrum of PSSS-VN is given in Figure 1 (curve a). The emission profile is similar to that previously reported for poly(2-vinylnaphthalene) sulfonate[8] with a monomer emission maximum at 335 nm and an intense broad excimer band at 382 nm. The emission profile of the aqueous PSSS-VN solution containing solubilized perylene is illustrated in Figure 1 (curve b). A comparison of the spectra shows that solubilization of perylene results in a decrease of naphthalene emission and the appearance of structured perylene emission in the 430–530 nm spectral region. This decrease in emission is due to energy transfer from excited pendant naphthalene groups to perylene and clearly indicates that perylene is trapped in the core of PSSS-VN. A comparison of the excitation spectrum ($\lambda_{em} = 480$ nm) of PSSS-VN, Figure 2 (curve a), with the photozyme (aqueous solution of PSSS-VN containing solubilized perylene), Figure 2 (curve b), is also in agreement with the above finding. The increased intensity observed in Figure 2 (curve b), between 230 and 335 nm, for direct excitation of naphthalene is a measure of the extent of singlet electronic energy transfer from excited naphthalene to perylene and therefore supports the conclusion that the probe is indeed trapped in the polymer core. Similar results have been obtained for DMA, DPA, MA, and A, indicating that these compounds

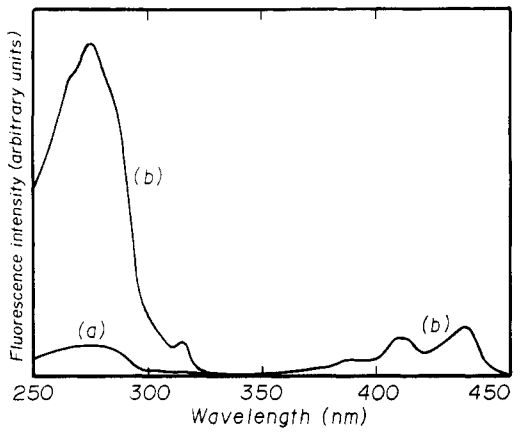

Figure 2. Excitation spectrum of PSSS (40 mol %)-VN in aqueous solution (a) and the corresponding spectrum of the system containing solubilized perylene (b) at neutral pH, λ_{em} = 480 nm, and $c_p^t = 1.07 \times 10^{-6}$ M.

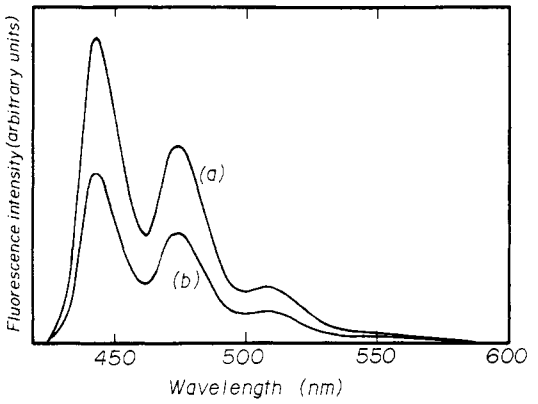

Figure 3. Fluorescence emission spectra of perylene solubilized in aqueous solutions of PSSS-VN containing 40 mol % SSS (a) and 47 mol % SSS (b) at neutral pH, λ_{ex} = 415 nm, and c_{pol} = 0.01 g dm^{-3}).

are also solubilized in the core of PSSS-VN.

I.a. Influence of the Polymer Composition, pH, and Ionic Strength on Solubilization. The solubilization of PNA compounds has been found to be dependent on the number of sulfonate groups in the polymer. Figure 3 shows the emission profile of perylene solubilized in an aqueous solution (at neutral pH) of PSSS (40 mol %)-VN (curve a) and PSSS (47 mol %)-VN (curve b) (c_{pol} = 0.01 g dm^{-3}). Solubilization of perylene is about 1.8 times more efficient in the polymer characterized by the lower number of sulfonate groups. This behavior is due to the greater repulsive interactions between adjacent ionic sulfonate groups in the polymer with a greater degree of sulfonation. Expansion of the polymer coil results in a less compact conformation and lowers the ability of the polymer to trap PNA compounds.

Another important variable which affects solubilization is the pH of the aqueous polymer solution. Figure 4 (curve a) shows the dependence of the total fluorescence intensity of perylene on the pH of the aqueous solution of PSSS-VN (c_{pol} = 0.4 g dm^{-3}). Measurements of the lifetime of perylene in its excited singlet state (Table I) indicate that a change in pH does not influence the quantum yield of fluorescence. Thus a change in the total fluorescence intensity reflects a difference in the concentration of probe solubilized in the polymer core. Inspection shows that maximum solubilization occurs at acid and alkaline pH, where the polymer coil is most compact (Figure 4, curve b). It can also be seen that solubilization of perylene is still quite effective at neutral pH.

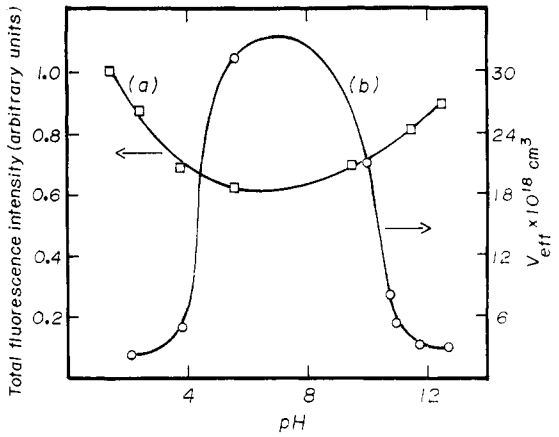

Figure 4. (a) Dependence of the total fluorescence intensity of perylene solubilized in aqueous solutions of PSSS (40 mol %)-VN (λ_{ex} = 415 nm) on pH and (b) dependence of the effective hydrodynamic volume of PSSS-VN on pH.

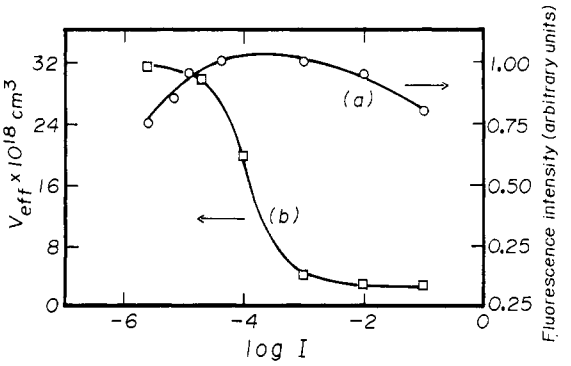

Figure 5. (a) Dependence of the total fluorescence intensity of perylene solubilized in aqueous solutions of PSSS-VN (λ_{ex} = 415 nm) on the ionic strength and (b) dependence of the hydrodynamic volume of PSSS-VN on the ionic strength.

Table I
Fluorescence Lifetime of Perylene (τ) Solubilized in Aqueous Solutions of PSSS-VN at Different Values of pH

pH	$\tau \pm 0.3$, ns
2	7.61
7	7.71
12	7.50

The change in pH results not only in a change in the acidity of the solution but also in a change of the ionic strength. The ionic strength effect was thus studied independently. An increase of the ionic strength in the range 10^{-6}–10^{-3} is accompanied by an increase of the solubilizing ability of the polymer. A further increase in the ionic strength, however, yielded a decrease in the amount of probe solubilized (Figure 5, curve a). This effect can be explained from the fact that an increase in the ionic strength results in a decrease of the repulsive interactions between sulfonate groups and causes the formation of a more compact coil as reflected by the decrease in the effective hydrodynamic volume (V_{eff}) (Figure 5, curve b). In the more compact conformation, the polymer solubilizes hydrophobic compounds more easily. Solubilization decreases, however, when the dimension of the polymer coil becomes too small.

I.b. Determination of the Distribution of PNA Compounds between Water and Polymer Pseudophase. In order to describe the solubilization of PNA compounds in aqueous solutions of PSSS-VN, it was assumed that the system could be treated as consisting of two phases, an aqueous phase and the polymer pseudophase.[10] The distribution coefficients of the PNA com-

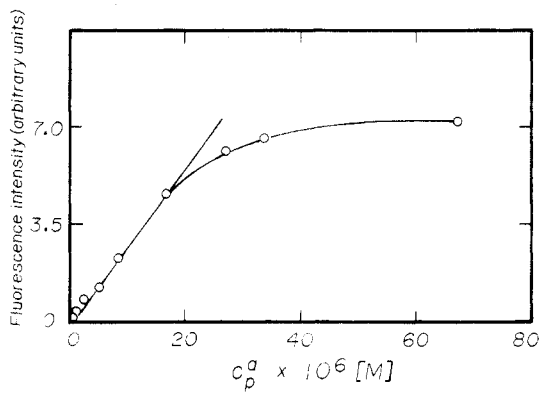

Figure 6. Dependence of the total fluorescence intensity of DPA (λ_{ex} = 354 nm) solubilized in aqueous solutions of PSSS-VN (c_{pol} = 0.5 g dm^{-3}) on the analytical concentration of DPA injected into the system.

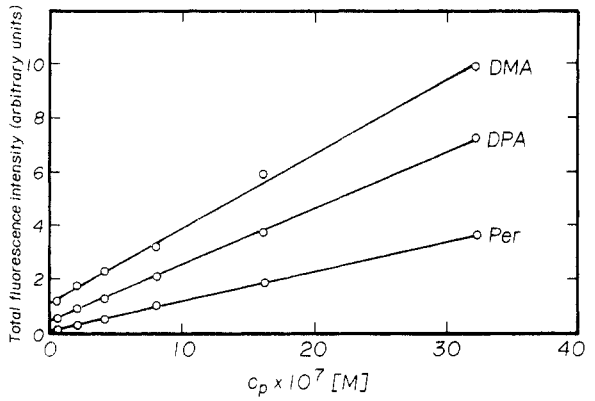

Figure 7. Dependence of the total fluorescence intensity of solubilized probes on the concentration of PSSS-VN.

pounds were determined in the saturated system. The amount of each probe needed to saturate the aqueous polymer solution was estimated from a plot of the dependence of the total emission intensity from direct excitation of the probe in the polymer solution (I_p^t) on the analytical concentration of probe injected (c_p^a) at the highest concentration of polymer used (c_{pol} = 0.5 g dm^{-3}). Figure 6 shows the dependence of I_p^t vs c_p^a for DPA. In the low concentration region an increase in the concentration of the probe added to the aqueous polymer solution is accompanied by a corresponding increase in the total fluorescence intensity of the probe (the linear part of the curve). A further increase in the analytical concentration of probe results in a slower increase of the total fluorescence of the system that eventually reaches a plateau. This indicates that the system is saturated under the experimental conditions. Using this procedure, it was possible to determine the amount of each probe needed to saturate the system.

The total fluorescence intensity of the probe saturated in a dilute solution of PSSS-VN increases considerably with an increase of the polymer concentration. In the polymer concentration range investigated, (0.5–35) × 10^{-7} M, a linear increase has been observed (Figure 7). It should be stressed that the total fluorescence represents a sum of emission from the probe present in the water phase and solubilized in the polymer pseudophase. Since the quantum yields of fluorescence of the probes in these two environments are expected to be different, it is difficult to determine the actual concentration of probe trapped in the polymer. The solubility of PNA compounds in water (c_{pol} = 0) is available in the literature.[19] The fluorescence intensity of the probe solubilized in the polymer solution

Table II
Values of the Parameters Characterizing the Solubilization of Some PNA Compounds in Aqueous Solutions of PSSS-VN at Neutral pH and Ionic Strength $I = 2 \times 10^{-6}$ [a]

probe	$10^{-7}K$ ± 5%	$10^6 c_p^t$, M	$10^2 c_p^c$, M	$10^6 c_p^{aq}$, M	n
A	12.70	18.60 ± 0.9	3.64 ± 0.18	0.37	6
DMA	15.80	11.10 ± 0.6	2.16 ± 0.04	0.27	3
DPA	36.70	6.40 ± 0.03	1.26 ± 0.03	0.10	2
MA	0.36	35.20 ± 1.7	6.76 ± 0.34	1.40	10
P	1870.00	2.18 ± 0.1	0.44 ± 0.02	0.0012	1

[a] K = distribution coefficients between polymer pseudophase and aqueous phase, c_p^t = total concentration of probe saturated in the polymer solution, c_p^c = concentration of probe in the polymer pseudophase, c_p^{aq} = concentration of probe in the saturated aqueous phase,[18] and n = average number of molecules of probe solubilized by one polymer macromolecule.

(especially at high polymer concentration) is expected to be dominated by emission from the polymer pseudophase. The total concentration (c_p^t) of a given probe can thus be calculated from a calibration curve obtained for the probe in an organic solvent. On the basis of these experimental data and with use of a modified form of the thermodynamic equations derived previously,[10] the mole fraction of the probe in the saturated aqueous phase (x_p^{aq}) and polymer pseudophase (x_p^c), the distribution coefficient (K) of the probe between the two phases, and the concentration of the probe in the polymer pseudophase (c_p^c) can be determined (see Table II)

$$c_p^t = 10^3 x_p^{aq}/M_{H_2O} + \frac{x_p^c}{1 - x_p^c}(c_{pol}) \quad (1)$$

$$c_p^{aq} = 10^3 x_p^{aq}/M_{H_2O} \quad (2)$$

$$K = x_p^c/x_p^{aq} \quad (3)$$

where c_{pol} is the polymer concentration and M_{H_2O} is the molecular weight of water.

The values of the distribution coefficient of the PNA compounds determined in this way are very high. They are summarized in Table II. It is apparent that the polymer efficiently solubilizes all of the PNA compounds investigated. Thus, even at a low concentration of probe in the system its local concentration is relatively high. The differences in the magnitude of the quantities (K, c_p^t, c_p^c) characterizing the solubilization of the probes in PSSS-VN solution leads to different values for the average number of probe molecules (n) per polymer macromolecule (see Table II). This variation arises from a difference in solubility of the probe in both phases, water and polymer pseudophase.

II. Photosensitized Reactions of PNA Compounds. II.a. Photochemical Reactions in a Nitrogen Atmosphere. Irradiation of the aqueous PSSS-VN solution, with light at λ = 280 nm, containing anthracene produced a decrease in the concentration of probe solubilized in the polymer core (Figure 8). The decrease is induced by electronic energy transfer from excited pendant naphthalene groups to the probe (as was shown in Figure 1) and appears to be due to photodimerization. The fact that no reduction of fluorescence emission was observed for DMA and DPA, although energy transfer to these probes occurs, supports the above suggestion. The photodimerization of the anthracene derivatives substituted at the 9,10-positions is considerably slower than for anthracene. For instance, the rate constant for photodimerization of DMA in benzene solution was found to be about two orders of magnitude lower than for anthracene in the same solvent.[20]

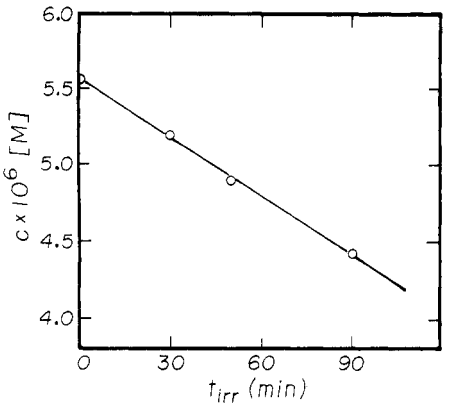

Figure 8. Change in the concentration of anthracene (A) during irradiation of the photozyme (λ_{irr} = 280 nm) in a nitrogen atmosphere.

Table III
Values of the Radius of Interaction between Pendant Naphthalene Groups in PSSS-VN and PNA Compounds

probe	R_0, Å
A	23.4 ± 0.3
MA	24.5 ± 0.3
DMA	25.9 ± 0.3
DPA	27.6 ± 0.4
P	31.2 ± 0.4

Electronic energy is transferred from pendant naphthalene chromophores to the PNA compounds according to the long-range Förster mechanism. The radius of interaction (R_0) was calculated by using the equation[21]

$$R_0^6 = \frac{8.8 \times 10^{-25} k^2 \phi_D}{n^4} \int_0^\infty F_D(\tilde{\nu})\, \epsilon_A(\tilde{\nu})\, (d\tilde{\nu}/\tilde{\nu}^4) \quad (4)$$

where ϵ_A is the extinction coefficient of the acceptor, F_D is the relative fluorescence intensity of the donor at $\tilde{\nu}$ satisfying $\int_0^\infty F_D(\tilde{\nu})\, d\tilde{\nu} = 1$, ϕ_D is the quantum yield of fluorescence of the donor in the absence of acceptor, $\int_0^\infty F_D(\tilde{\nu})\, \epsilon_A(\tilde{\nu})\, d\tilde{\nu}$ is the overlap integral between the emission profile of the donor and the absorption spectrum of the acceptor, k^2 is the molecular orientation factor, and n is the refractive index of the solvent. The values of R_0 for each probe are given in Table III.

The dimerization of anthracene has been shown to occur via the formation of an excimer intermediate:[22,23]

$$^1A^* + {}^1A_0 \rightarrow [{}^1A^*{:}{}^1A_0] \rightarrow A\text{–}A \quad (5)$$

One would expect a dimerization reaction when anthracene molecules are in close proximity. This condition seems to be fulfilled in the anthracene-saturated aqueous polymer solution. Calculations of the mole fraction of anthracene in such a solution give a value of $x_p^c = 0.86$. Thus statistically, one polymer coil is capable of solubilizing about six anthracene molecules. This explains why dimerization occurs easily in anthracene-saturated solutions of PSSS-VN. Figure 9a displays the fluorescence spectra of anthracene (λ_{ex} = 340 nm) solubilized in aqueous PSSS-VN solutions at a total concentration of anthracene equal to 18.6×10^{-6} M (curve a) and 2.69×10^{-6} M (curve b). The spectra were recorded at 77 K, and the fluorescene intensity was normalized to the peak maximum at 401 nm. Saturation of the aqueous PSSS-VN solution with anthracene resulted in an increase in the long-wavelength part of the spectrum. This effect is believed to be due to the formation of anthracene excimer. This conclusion is based on a comparison of the emission profile of anthracene in PSSS-VN to the fluorescene spectrum of anthracene excimer reported in cyclohexane at 20 K.[24] The fluorescence at and below 401 nm is due to monomer emission, while that observed at longer wavelengths represents a sum of monomer and excimer emission.[24] It is obvious that the probability of excimer formation is considerably higher in the more concentrated anthracene solution. As previously mentioned an average of six anthracene molecules are solubilized per polymer coil for the saturated system compared to less than one for the dilute solution. It was very difficult to compare the spectra in a quantitative way. The increase in the hydrophobicity of the microdomains induced by a greater amount of anthracene solubilized in the polymer core resulted in a shift of the fluorescence maxima and a change in the half-widths of the spectral bands. Subtraction of the spectra (Figure 9A) in the long-wavelength spectral region yielded the spectrum of anthracene excimer shown in Figure 9B. The spectrum agrees quite well with that previously reported for anthracene excimer in cyclohexane at 77 K.[24] Figure 9C illustrates the dependence of the ratio of excimer (448 nm) to monomer (401 nm) fluorescence of anthracene on the total concentration of anthracene solubilized in the aqueous PSSS-VN solution. It can be seen that an increase in the concentration of anthracene resulted in an increase in the probability of excimer formation.

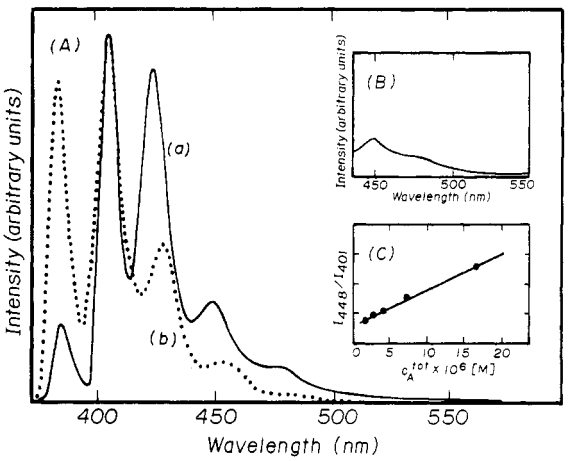

Figure 9. (A) Emission of anthracene from an aqueous solution of PSSS-VN (λ_{ex} = 340 nm, T = 77 K, c_p = 0.5 g dm^{-3}) at a concentration of 18.6×10^{-6} M (a) and 2.69×10^{-6} M (b). (B) Emission of anthracene excimer recorded at 77 K. (C) Dependence of the ratio of I_{448}/I_{401} on the total concentration of anthracene.

In the case of the photosensitized dimerization process observed in the photozyme (λ_{ex} = 280 nm) the formation of the excimer intermediate is expected to be induced by energy transfer from the excited pendant naphthalene polymeric units to anthracene. The quantum efficiency of dimerization (γ_{Dim}) can be thus described by the equation

$$\gamma_{Dim} = \phi_{ET}\phi_{Dim} \quad (6)$$

where ϕ_{ET} and ϕ_{Dim} are the quantum yields of energy transfer and dimerization, respectively. The quantum efficiency of dimerization of anthracene saturated in the aqueous solution of PSSS-VN ($c_p^c = 3.5 \times 10^{-2}$ M) has been determined to be equal to 1×10^{-3}.

II.b. Photooxidation of Polynuclear Aromatic Compounds. Irradiation of the photozyme (PSSS-VN + probe) in the presence of oxygen resulted in a rapid decrease in the fluorescence of PNA compounds (Figure 10). The decrease in emission is due to photooxidation of the probes. It is well-known that the photooxidation of PNA compounds occurs with participation of singlet oxygen.[11-14] The reaction could be easily monitored by the decrease of

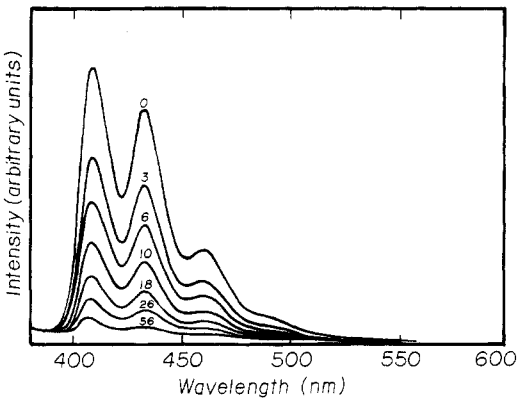

Figure 10. Decrease in the fluorescence emission of DMA (λ_{ex} = 356 nm) solubilized in PSSS-VN for various irradiation times (minutes).

Table IV
Secondary Products Detected during Thermolysis of Primary Oxidation Products in Photozyme

type of photozyme	product	detection method
PSSS-VN + DPA	DPA	fluorescence, GC
	$^1O_2$	fluorescence (via reaction with DPBF)
PSSS-VN + A	anthraquinone	GC
PSSS-VN + DMA	anthraquinone	GC
	10-methyl-10-hydroxy-anthrone	GC

fluorescence, as the PNA compounds were transformed to the nonemitting endoperoxides. The typical, well-known reaction of DMA is illustrated below.

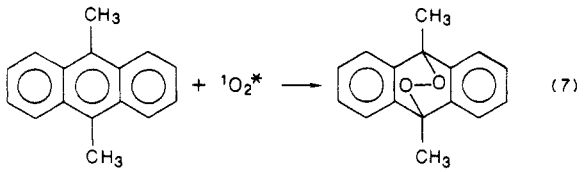

The photooxidation products of PNA compounds in the photozyme were detected by gas chromatography. The products were compared with those formed during dye-sensitized (Rose Bengal) and self-sensitized oxidation of the PNA compounds in methanol and benzene solution, respectively. It was not possible to detect the endoperoxides directly because of their relatively low thermal stability. The type of secondary products, however, indicated that endoperoxides had to be considered as the primary photooxidation products (see Table IV). Model studies have shown that the thermolysis products of endoperoxides of PNA compounds depend on the type of PNA compound oxidized.[25-30] Also, the relative yield of the different products is sensitive to a change in the temperature and the type of solvent used.[25,29]

The decomposition of the endoperoxide of DPA resulted in the formation of DPA and singlet oxygen. The activation energy of the process was estimated to be equal to 27.8 ± 0.2 kcal mol^{-1}.[27] Heating of the photozyme consisting of oxidized DPA for 15 h at 90 °C yielded an increase of DPA emission of about 10%. Thermolysis in the presence of the known singlet oxygen acceptor, 1,3-diphenylisobenzofuran (DPBF), for 30 min produced a 75% decrease in the fluorescence intensity of DPBF solubilized in the polymer microphase. This decrease is mainly due to the oxidation of DPBF with singlet oxygen and provides additional evidence for the generation of singlet oxygen upon thermolysis of DPA. In a control experiment it was found that the reaction of DPBF with molecular oxygen

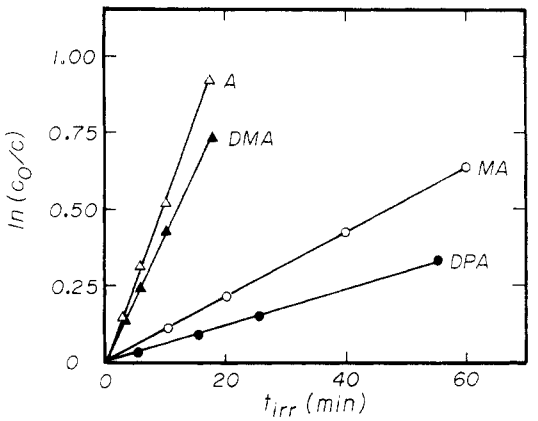

Figure 11. Dependence of ln (c_0/c) on irradiation time (t) for photooxidation of probes in photozyme: c_0, initial concentration of probe; c, concentration of probe at time t.

in the ground state is about seven times slower than in the photozyme system.

Anthraquinone was identified during GC analysis of the photooxidation products in the photozyme containing anthracene and is known to be a compound created during thermal decomposition of anthracene endoperoxide.[28,29] The activation energy for oxygen–oxygen bond homolysis in anthracene endoperoxide has been estimated to be 29.8 kcal mol^{-1}.[30]

Thermolysis of the endoperoxide of DMA gives several molecular products, including anthraquinone and 10-methyl-10-hydroxyanthrone,[25,29] which were also identified as secondary products formed during oxidation of photozyme containing DMA.

The photooxidation of PNA compounds in the photozyme can be described by a pseudo-first-order kinetic equation up to a relatively high degree of conversion (Figure 11). Singlet oxygen can be formed from oxygen quenching the electronically excited states of both naphthalene and probe. Since the concentration of probe molecules in the electronically excited states is considerably lower than the excited pendant naphthalene groups, PNA participation in singlet oxygen formation can probably be neglected.

The following kinetic scheme for photooxidation of PNA compounds in aqueous PSSS-VN solution can be proposed:

$$^1N_0 + h\nu \rightarrow {}^1N^* \quad (8)$$

$$^1N^* \underset{k_F}{\xrightarrow{k_{IC}}} {}^1N_0 \quad (9)$$

$$^1N^* + {}^1N_0 \xrightarrow{k_1} {}^1Ex \quad (10)$$

$$^1N^* \xrightarrow{k_{ISC}} {}^3N^* \quad (11)$$

$$^1N^* + {}^3O_2 \xrightarrow{k_q^S} {}^3N^* + {}^1O_2^* \quad (12a)$$

$$^1N^* + {}^3O_2 \xrightarrow{k_q} {}^3N^* + {}^3O_2 \quad (12b)$$

$$^1N^* + {}^1P_0 \xrightarrow{k_{ET}} {}^1N_0 + {}^1P^* \quad (13)$$

$$^3N^* + {}^3O_2 \xrightarrow{k_q^T} {}^1N_0 + {}^1O_2 \quad (14)$$

$$^1P_0 + {}^1O_2^* \xrightarrow{k_r} PO_2 \quad (15)$$

$$^1O_2^* \xrightarrow{k_d} {}^3O_2 \quad (16)$$

where the symbols $^1N_0$, $^1N^*$, and $^3N^*$ are for the pendant naphthalene groups in the ground, excited singlet, and excited triplet states, respectively, $^3O_2$ and $^1O_2^*$ represent

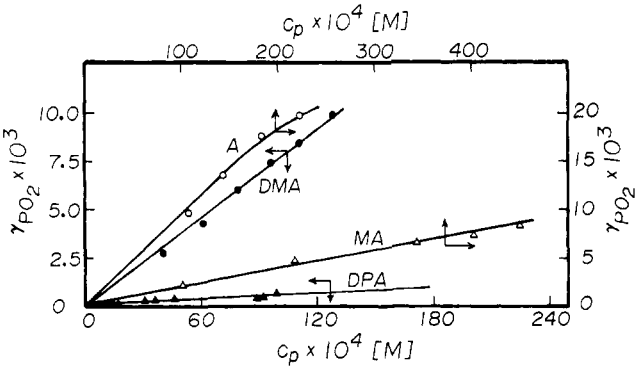

Figure 12. Dependence of the quantum efficiency of photooxidation of probes (γ_{PO_2}) on concentration of probe in the polymer pseudophase (c_p^c).

oxygen in the ground and excited singlet state, respectively, $^1P_0$ is a molecule of probe (PNA), and PO_2 is the endoperoxide product.

The quantum efficiency of photooxidation (γ_{PO_2}) of the PNA compounds investigated can be given by the equation

$$\gamma_{PO_2} = \gamma_\Delta \phi_{PO_2} \tag{17}$$

where γ_Δ is the quantum efficiency of singlet oxygen formation and ϕ_{PO_2} is the quantum yield of reaction between singlet oxygen and probe. The quantum yield of reaction between $^1O_2$* and probe can be given by the equation

$$\phi_{PO_2} = \frac{k_r[P]}{k_r[P] + k_d} \tag{18}$$

where k_r is the rate constant of reaction, k_d is the rate constant for radiationless decay of singlet oxygen, and P is the concentration of the probe.

Substitution of eq 18 into eq 17 yields the analytical form of the dependence of the quantum efficiency of photooxidation on the concentration of probe:

$$\gamma_{PO_2} = \gamma_\Delta \left(\frac{k_r[P]}{k_r[P] + k_d} \right) \tag{19}$$

Since the lifetime of singlet oxygen in the liquid phase is relatively short, one would expect the reaction between PNA compounds and $^1O_2$* to occur in the interior of the polymer, where singlet oxygen is formed. Thus the quantum efficiency of photooxidation is dependent not on the total concentration of probe present in the system but on the local concentration in the polymer pseudophase. From a knowledge of the concentration of probe injected into the system and the previously determined values of the distribution coefficients, the concentration of probe solubilized in the polymer pseudophase can be calculated. The differences in solubilities and distribution coefficients of the PNA compounds results in considerable variations in the local concentration of probe in the polymer core. Figure 12 shows the dependence of the quantum efficiency of photooxidation of PNA compounds on the concentration of PNA in the polymer microphase.

In order to compare the reactivity of the probes the values of the quantum efficiency of photooxidation, at the same concentration in the polymer pseudophase, were determined (Table V).

The values of γ_{rel} for the photosensitized oxidation of PNA compounds with $^1O_2$* in aqueous solutions of PSSS-VN correspond to the same trend observed for these substances in benzene solution.[14] The higher than expected value of the quantum efficiency of anthracene consumption can be rationalized considering the possible occurrence of two types of reactions, oxidation and dimerization, taking place simultaneously. Although the dimerization process should be retarded in the presence of oxygen, it is not expected to be completely eliminated. The exceptionally high local concentration of solubilized anthracene favors the dimerization process.

Table V
Quantum Efficiencies of Photooxidation of Probes (γ_{PO_2}) at the Same Local Concentration (c_p^c) and the Respective Relative Values (γ_{rel})

probe	$10^3\gamma_{PO_2}$	γ_{rel}
DMA	7.7 ● 0.4	1.0
MA	2.0 ± 0.2	0.26
DPA	0.6 ± 0.1	0.08
A	10.0 ± 0.5	1.3

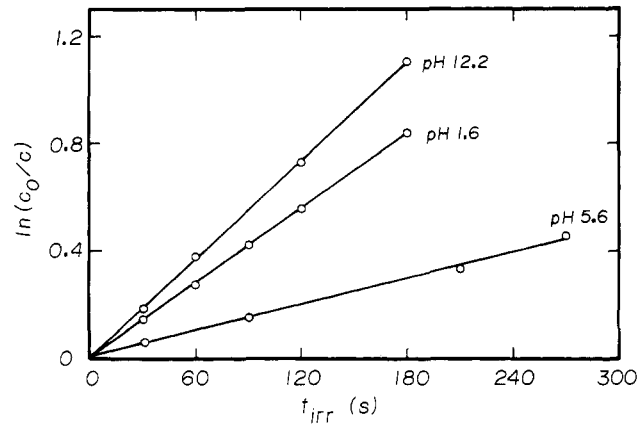

Figure 13. Kinetics of DMA photooxidation at three different pH values.

Interestingly, the rate of photooxidation of probe molecules, determined at the same total concentration of probe, was found to be dependent on the pH of the aqueous polymer solution. Figure 13 shows the dependence of ln (c_0/c) vs irradiation time for photooxidation of DMA at three different pH values. The reaction was found to be 2.3 times faster at pH 1.6 and 3.8 times faster at pH 12.2 than at neutral pH. This effect can be explained from the fact that pH induces a change in the size of the polymer core (compare Figure 4). In the acidic and alkaline regions, the polymer core is much more compact than at neutral pH. It is believed that the compact polymer core affects the photooxidation process in two ways. First, the distance between singlet oxygen and the probe is smaller. Second, the compact coil has microdomains with more hydrophobic character in which oxygen solubility should be greater. Thus a higher concentration of singlet oxygen should be generated, and the probability of oxygenating probe molecules during the lifetime of $^1O_2$* should increase. The result of this experiment strongly supports the thesis that the reaction takes place in the interior of the polymer core.

II.c. Photochemical Reactions Initiated by Solar-Simulated Radiation. The possible practical applications of PSSS-VN as a photocatalyst for oxidation of PNA compounds in aqueous solution was studied by using solar-simulated light. Photooxidation of PNA compounds was found to be very efficient under these experimental conditions (see Figure 14). In order to compare the efficiency of photoreaction in the photozyme to the reaction in organic solvent the irradiation of DMA in aqueous PSSS-VN and in benzene solution, at an identical initial concentration of DMA (3.9×10^{-6} M), was performed. The photooxidation of DMA was found to be faster in the photozyme than in benzene solution. The rate constants for the pseudo-first-order photooxidation of DMA after

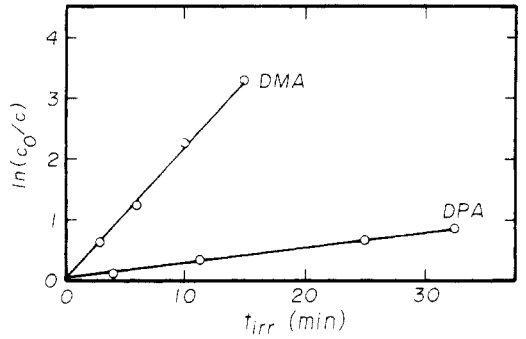

Figure 14. Dependence of ln (c_0/c) on irradiation time for photooxidation of DMA and DPA in the photozyme with solar-simulated radiation.

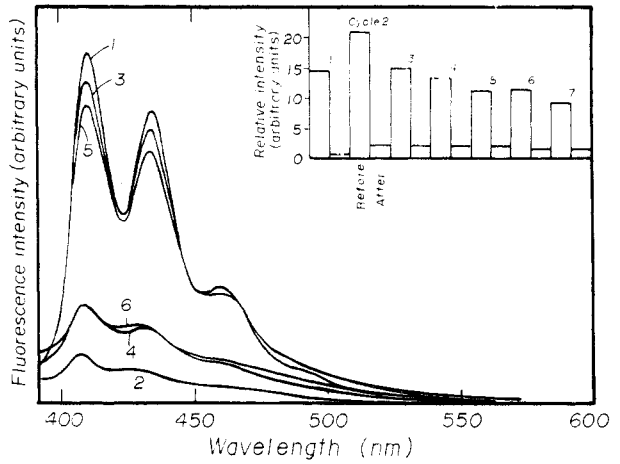

Figure 15. Changes in fluorescence spectra of DMA in photozyme (λ_{ex} = 356 nm) recorded for three cyclic processes and a bar graph of the changes in the fluorescence intensity of DMA before and after irradiation for seven cycles. Each cycle involves solubilization and irradiation of the photozyme for 15 min with solar-simulated light. Spectral curves 1 and 2 are recorded before and after irradiation in cycle 1, curves 3 and 4 in cycle 4, and curves 5 and 6 in cycle 6.

20 min of irradiation in the photozyme and in benzene were observed to be 0.44 and 0.16 min^{-1}, respectively. The difference in the rate of reaction in these two media increases with a decrease in the concentration of probe in the system. At lower probe concentrations the self-sensitized photooxidation of DMA is less probable than photooxidation sensitized by the polymer. This effect is due to the increasing difference in the optical density of the two systems as well as the difference in the concentration of probe. Although the total concentration of DMA in both systems is identical, the local concentration participating in the reaction is considerably higher in the PSSS-VN solution. This result should be important in considering the potential photocatalytic applications of PSSS-VN.

PSSS-VN was also found to exhibit other interesting features. It is photostable under the experimental conditions. It can be used as a photocatalyst several times. After photooxidation, the polymer is able to solubilize more probe and photooxidation could be repeated (Figure 15). However, after several irradiation cycles solubilization decreases, but photooxidation is still efficient (compare bar graph in Figure 15). Thus the polymer can be used in a cyclic process.

Conclusions

Aqueous solutions of PSSS-VN efficiently solubilize sparingly water-soluble large hydrophobic polynuclear aromatic compounds. Solubilization is enhanced in acidic and alkaline solutions. This behavior is connected with an increase in the compactness of the polymer core in both these regions.

The solubilized probes are capable of accepting electronic excitation from the polymer. The energy-transfer process probably occurs according to the Förster long-range resonance mechanism. In the absence of oxygen anthracene was found to undergo photodimerization. In the presence of oxygen, however, energy transfer to $^3O_2$ results in the formation of singlet oxygen. Singlet oxygen reacts with the PNA compounds to form nonemitting endoperoxides.

The photooxidation of PNA compounds has been found to be also very efficient during irradiation of the photozyme with solar-simulated radiation. It has been shown that the solubilization and photooxidation can be performed in a cyclic manner, which may be important for practical application of PSSS-VN as a photocatalyst.

Acknowledgment. The financial support of this research by the Natural Sciences and Engineering Research Council of Canada and the Ontario Centre for Materials Research is gratefully acknowledged. J.E.G. is grateful to the Canada Council for support in the form of a Killam Research Fellowship.

Registry No. PSSS-VN (copolymer), 115468-37-6; DMA, 781-43-1; DPA, 1499-10-1; MA, 779-02-2; A, 120-12-7; P, 198-55-0; DPBF, 5471-63-6; anthraquinone, 84-65-1; 10-hydroxyanthrone, 549-99-5.

References and Notes

(1) Barone, G.; Crescenzi, V.; Liquori, A. M.; Quadrifoglio, F. *J. Phys. Chem.* **1967**, *71*, 2341.
(2) Treloar, F. E. *Chem. Scr.* **1976**, *10*, 219.
(3) Tan, K. L.; Treloar, F. E. *Chem. Phys. Lett.* **1980**, *73*, 234.
(4) Dubin, P., Ed. *Microdomains in Polymer Solutions*; Plenum Press: New York, 1985.
(5) Molyneux, P. *Water Soluble Polymers; Properties and Behaviour*; CRC Press: Boca Raton, FL, 1984; Vol I, II.
(6) Holden, D. A.; Rendall, W. A.; Guillet, J. E. *Ann. N.Y. Acad. Sci.* **1981**, *366*, 11.
(7) Guillet, J. E.; Rendall, W. A. *Macromolecules* **1986**, *19*, 224.
(8) Guillet, J. E.; Wang, J.; Gu, L. *Macromolecules* **1986**, *19*, 224.
(9) Nowakowska, M.; White, B.; Guillet, J. E. *Macromolecules* **1988**, *21*, 3430.
(10) Nowakowska, M.; White, B.; Guillet, J. E., submitted for publication in *Macromolecules*.
(11) Gollnick, K. *Adv. Photochem.* **1968**, *6*, 1.
(12) Gollnick, K. In *Singlet Oxygen*; Rånby, B., Rabek, J. F., Eds.; Wiley: New York, 1978.
(13) Stevens, B.; Algar, B. E. *J. Phys. Chem.* **1968**, *72*, 2582.
(14) Stevens, B.; Perez, S. R.; Ors, J. A. *J. Am. Chem. Soc.* **1974**, *96*, 6846.
(15) Carlson, S. A.; Hercules, D. M. *Anal. Chem.* **1973**, *45*, 1794.
(16) Parker, C. A. *Photoluminescence of Solutions*; Elsevier: New York, 1968.
(17) Kilp, T.; Houvenaghel-Defoort, B.; Panning, W.; Guillet, J. E. *Rev. Sci. Instrum.* **1976**, *47*, 1496.
(18) Patterson, L. K.; Vieil, E. *J. Phys. Chem.* **1973**, *77*, 1191.
(19) Pearlman, R. S.; Yalkowsky, S. H.; Banerjee, S. *J. Phys. Chem. Ref. Data* **1984**, *13*, 555.
(20) Bouas-Laurent, H.; Castellan, A.; Desvergne, J.-P. *Pure Appl. Chem.* **1980**, *52*, 2633.
(21) Guillet, J. E. *Polymer Photophysics and Photochemistry*; Cambridge University Press: Cambridge, 1985.
(22) Yang, N. C.; Shold, D. M.; Kim, B. *J. Am. Chem. Soc.* **1976**, *98*, 6587.
(23) Cohen, M. D.; Ludmer, A.; Yakhot, V. *Chem. Phys. Lett.* **1976**, *38*, 398.
(24) Ferguson, J. *J. Chem. Phys.* **1965**, *43*, 307.
(25) Rigaudy, J.; Moreau, M.; Cuong, N. K.; Normant, M. H. *C. R. Acad. Sci. Paris, Ser. C* **1972**, *274*, 1589.
(26) Southern, P. F.; Waters, W. A. *J. Chem. Soc.* **1960**, 4340.
(27) Wasserman, H. H.; Scheffer, J. R.; Cooper, J. L. *J. Am. Chem. Soc.* **1972**, *94*, 4991.
(28) Aspler, J.; Carlsson, D. J.; Wiles, D. M. *Macromolecules* **1976**, *9*, 691.
(29) Rigaudy, J.; Baranne-Lafont, J.; Defoin, A. *Tetrahedron* **1978**, *34*, 73.
(30) Breitenbach, J. W.; Kastell, A. *Monatsh. Chem.* **1954**, *85*, 676.